# Proposal of a New Tool for Pre-Straining Operations of Sheet Metals and an Initial Investigation of CR4 Mild Steel Formability

# Proposal of a New Tool for Pre-Straining Operations of Sheet Metals and an Initial Investigation of CR4 Mild Steel Formability

**A Barlo[1,*], M Sigvant[1,2], M S Islam[1], Ll Pérez[3], E Olofsson[4], M Al-Fadhli[5], Q T Pham[1], J Pilthammar[1,2], E-L Odenberger[3]**

[1]Dept. of Mechanical Engineering, Blekinge Institute of Technology, Karlskrona, Sweden
[2]Volvo Cars Dept. 81110 Strategy Development, Olofström, Sweden
[3]RISE Research Institutes of Sweden, Component Manufacturing Unit, Olofström, Sweden
[4]Volvo Cars Dept. 81253 Commodity Hang on Parts, Gothenburg, Sweden
[5]Volvo Cars Dept. 81151 Product & Process Structures, Olofström, Sweden

E-mail: Alexander.Barlo@bth.se

**Abstract.** With the increased focus on reducing carbon emissions in the automotive industry, more advanced materials are introduced to reduce the vehicle weight, and more complex component geometries are designed to both satisfy customer demands and to optimize the vehicle aerodynamically. With the increase in component complexity, the strain paths produced during the forming operation of car body components often display a highly non-linear behavior which makes the task of failure prediction during the manufacturing feasibility studies more difficult. Therefore, CAE engineers need better capabilities to predict failure induced by strain path nonlinearity. This study proposes a new tool designed for creating bi-linear strain paths, by performing a pre-strain of a sheet large enough to cut out Nakajima specimens to perform the post-straining in any direction. From five pre-straining tests the tool present a stable pre-straining operation with a uniform strain field in a radius of 100 [mm] from the centre, corresponding to the region of interest of a Nakajima specimen. From the five pre-strained samples, different Nakajima specimens are cut transverse and longitudinal to the rolling direction and a failure prediction approach in an alternative, path independent evaluation space was used to predict the onset of necking with promising results.

## 1. Introduction

With an increased focus on carbon emission reduction in today's society, more and more advanced material grades of sheet metals are introduced to the market. This, combined with the consumers increasing demand for complex products, creates a number of challenges in the sheet metal forming industry. One already existing challenge amplified by these demands is the presence of non-linear strain paths during the forming process. For several decades, this particular issue has been targeted by multiple authors, including Stoughton [1], Volk and Suh [2], and Mattiason et al. [3]. With the recent changes driven by demand, the severity of the path non-linearity also increases. Recently, both Norz et al. [4] and Barlo et al. [5] tested different numerical approaches to predict failure in an automotive component with a critical element displaying a strain path with a radical change in the loading direction - both not successfully. This paper proposes a new tool geometry for the pre-straining of sheets and sets

out to investigate an alternative evaluation space for the prediction of failure caused by non-linear strain paths. The tool consists of three parts - a punch, a binder, and a die. The punch has a size of $598 \times 398$ [mm] with rounded edges and a shoulder radius of 25 [mm]. The die has an opening of $603.7 \times 403.5$ [mm] with a die radius of 10 [mm]. To restrain the material during the forming operation, draw beads with a bead height of 6 [mm] and shoulder radius of 4 [mm] are used. An illustration of the entire tool and a picture of the punch can be found in Figure 1.

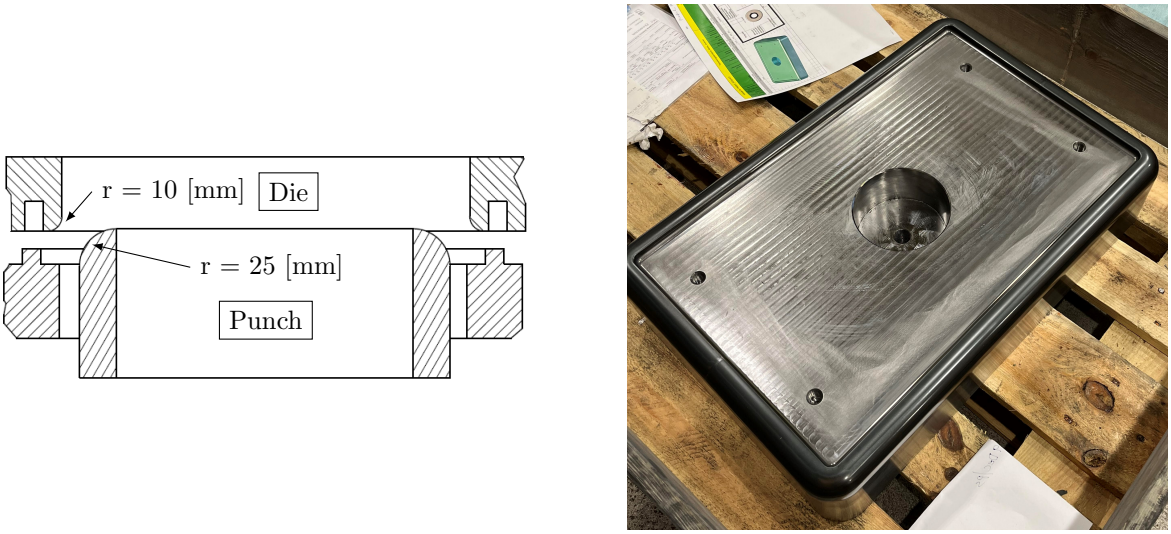


**Figure 1:** Cross-section of entire tool geometry and the manufactured punch.

The tool is designed to provide a pre-straining with a uniform strain distribution in the centre of the sheet in a circular area with a diameter of 200 [mm]. With the uniform strain distribution in this area, the full range of Nakajima specimens according to ISO-12004 [6] can be cut from the blank allowing for the determination of a pre-strain Forming Limit Curve (FLC). This process is outlined in Figure 2.

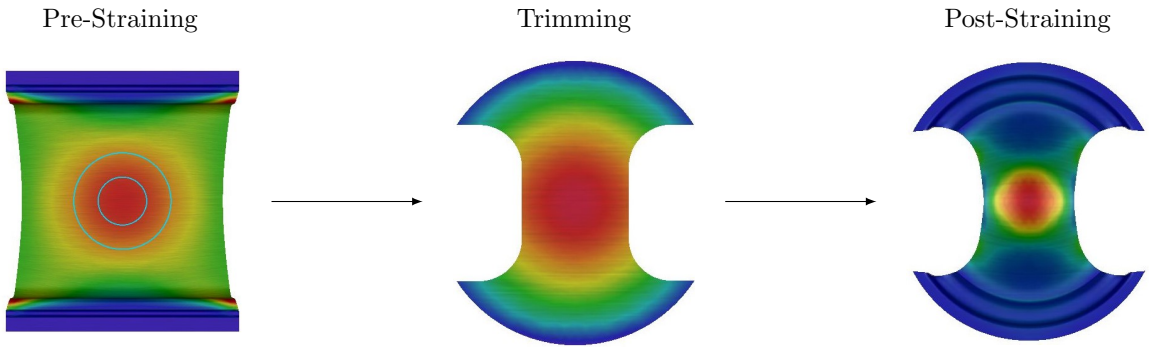


**Figure 2:** Proceedure of the bi-linear straining operation exemplified by the pre-straining of the $480 \times 550$ [mm] blank and post-straining of a Nakajima 75 sample. The circles presented on the pre-straining outlines the 200 [mm] diameter of the Nakajima full width blank, and the 100 [mm] diameter of the Nakajima punch serving as the region of interest for the DIC analysis.

## 2. Experimental Work

To perform the initial investigation, five rectangular 480 × 550 [mm] blanks were cut to obtain straining transverse to the rolling direction. For the pre-straining, the cut blanks were stretch to a punch depth of 62.6 [mm] with a ram velocity of approximately 22 [mm/s]. To reduce the friction in the forming operation, a suitable lubrication system was applied between the tool parts and blank. For the determination of the pre-straining levels, ARGUS measurements were performed, where the average major and minor strains of a Ø100 [mm] circle in the centre of the formed blank (see inner circle highlighed on Figure 2) were determined as the pre-straining levels, and can be found in Table 1.

For the post-straining, five different Nakajima test geometries were cut from the pre-strained blanks: 75, 100, 125, and 200 samples transverse to the rolling direction, and a 125 sample longitudinal to the rolling direction. The Nakajima tests were performed according to the ISO 12004-2 standard [6], and the strain fields were captured by a 3D ARAMIS DIC system. The determined mode of failure for the Nakajima post-straining samples was the onset of necking, and the method proposed by Sigvant et al. [7] was used to determine the necking strain limits. The determined limit strains for the post-straining operations of the 5 samples can be found in Table 1.

**Table 1:** Pre- and post-straining strain values. PS_XX test numbers indicate pre-straining, and the Nakajima sample size are presented followed by either T for transverse or L for longitudinal indicating the rolling direction relative to the major straining direction for the post-straining operations.

| Pre-Straining | | | Post-Straining | | |
|---|---|---|---|---|---|
| Test No | $\varepsilon_2^{pre}$ | $\varepsilon_1^{pre}$ | Specimen | $\varepsilon_2^{post}$ | $\varepsilon_1^{post}$ |
| PS_01 | -0.197 | 0.306 | 75T | -0.065 | 0.164 |
| PS_02 | -0.198 | 0.306 | 100T | -0.008 | 0.082 |
| PS_03 | -0.193 | 0.300 | 125T | 0.005 | 0.059 |
| PS_04 | -0.197 | 0.306 | 125L | 0.002 | 0.053 |
| PS_05 | -0.192 | 0.297 | 200T | 0.161 | 0.168 |

Based on the strain values presented, a new FLC can be generated based on the pre-strained samples. Figure 3 presents the new FLC based on the four Nakajima specimens tested in the transverse direction. For the case of the 125L specimen, this experiment was performed to replicate the strain path investigated by Norz et al. [4] and Barlo et al. [5], where a radical change in strain direction is seen. For the strain path presented in Figure 3 representing the 125L sample, the change in loading direction results in the minor strain of the post-straining operation being added to the major strain of the pre-straining and the major strain of the post-straining to the minor strain of the pre-straining.

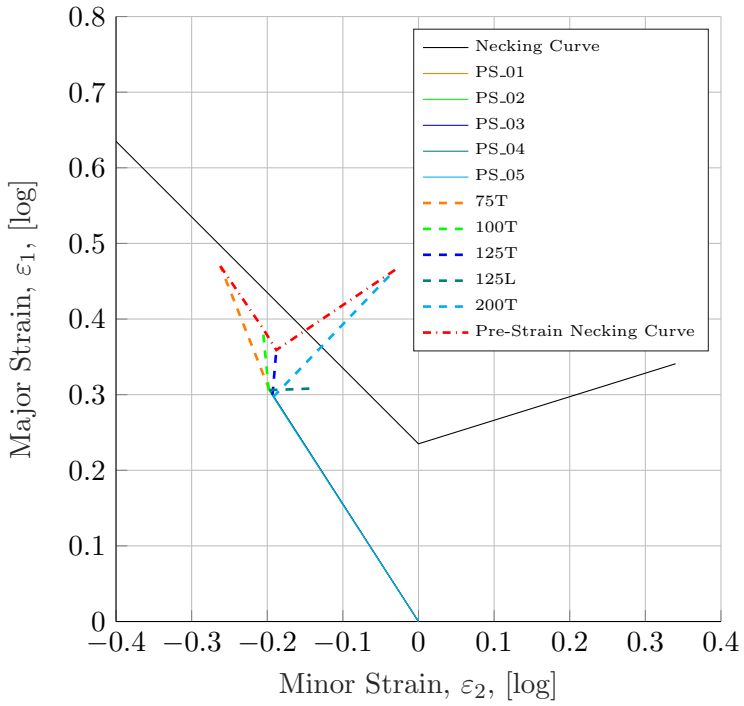


**Figure 3:** Forming Limit Curve generated from the pre-strained Nakajima specimens. The specimen 125L is not used as a data point in the limit curve, as the testing direction is different from the pre-straining.

The experimental results presented in Table 1 and Figure 3 shows that the presented tool produce stable pre-straining to the tested geometry. Therefore, an initial investigation of the ability to predict non-linear failure in the specimens tested can be performed.

## 3. Failure Prediction of Bi-Linear Strain Paths

For the initial investigation of failure prediction, the methodology proposed by Zeng et al. [8] for prediction of failure due to non-linear strain paths was used. In this methodology, a transformation of the standard forming limit diagram to a new evaluation space defined by the material flow direction $\alpha$ and the effective plastic strain $\bar{\varepsilon}^p$ is performed. In this initial investigation, an assumption of linear and proportional deformation ($d\varepsilon_i = \varepsilon_i$) is made for the pre- ($0 \rightarrow \varepsilon_i^{pre}$) and post-straining ($\varepsilon_i^{pre} \rightarrow \varepsilon_i^{post}$) strain paths.

In order to apply the methodology, inverse modeling of the experiments was performed, as the effective plastic strain cannot be obtained from DIC. For the inverse modeling, Finite Element models were built in AutoForm™ R10 using the BBC2005 material model. The input parameters for the material model can be found in Table 2, and the yield surface and hardening curve can be found in Figure 4.

**Table 2:** BBC2005 material input for the VDA239 CR4 mild steel. The exponent $M = 2k$ in the BBC2005 deviates from the crystallographic determined values, with the presented valued having been determined through inverse modeling to obtain a more accurate principal strain prediction [9].

| $r_0$ | $r_{45}$ | $r_{90}$ | $r_b$ | $\sigma_0/\sigma_0$ | $\sigma_{45}/\sigma_0$ | $\sigma_{90}/\sigma_0$ | $\sigma_b/\sigma_0$ | M |
|---|---|---|---|---|---|---|---|---|
| 1.805 | 1.336 | 1.876 | 0.982 | 1 | 1.0214 | 0.9959 | 1.1938 | 4.5 |

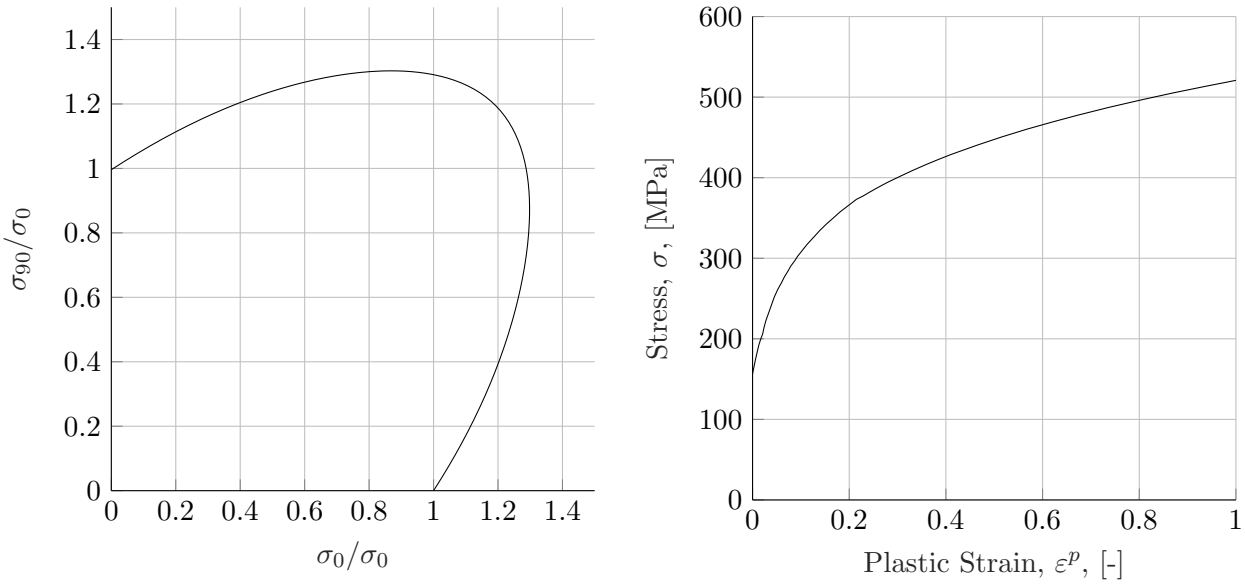


**Figure 4:** Yield surface and hardening curve of the VDA239 CR4 mild steel.

To replicate the friction conditions in the pre-straining experiment caused by the lubrication system, a mixed approach is taken using both Coulomb and Triboform® friction models. For the forming of the Nakajima specimens, an identical approach to eliminate friction was taken. Table 3 presents the different friction models applied to different areas of the model.

**Table 3:** Friction model setup of Finite Element Model.

| **Tool Part** | **Friction Model** | **Friction Coefficient, $\mu$, [-]** |
|---|---|---|
| Die | Coulomb | 0.15 |
| Binder | Coulomb | 0.15 |
| Punch | Coulomb | 0.01 |
| Die Radius | TriboForm | - |

With the described setup there are deviations between the experimental and simulated force-displacement responses, see Figure 5. For the pre-straining operation, there is an acceptable fit between the experiments and simulation up to 30 [mm] of punch displacement. After this, the simulation starts to drift, and overestimates the maximum force by approximately 20 [kN]. For the post-straining operation, the fit of the simulation varies between the Nakajima samples. An acceptable fit is seen for both the 75T and 100T samples, a slightly less accurate fit is seen for the 125T and 125L samples, and finally an even less accurate fit for the 200T sample. For this initial investigation, these fits are however deemed acceptable, as for the majority of cases in the post-straining (except the 200T sample) the major part of the deviation occurs after the point determined to be the onset of necking.

With the calibrated models, the effective plastic strain value $\bar{\varepsilon}^p$ was determined by identifying the punch displacement in the simulation corresponding to the onset of necking identified in the experimental analysis of the post-straining operation. In the determined step, the element with the maximum major strain was identified and corresponding effective plastic strain values were found. To assess the quality of the investigated method, a comparison to the Advanced Formability option in AutoForm™ R10 (based on the Generalized Forming Limit Concept (GFLC) proposed by Volk and Suh [2]) was made. The Advanced Formability assessment

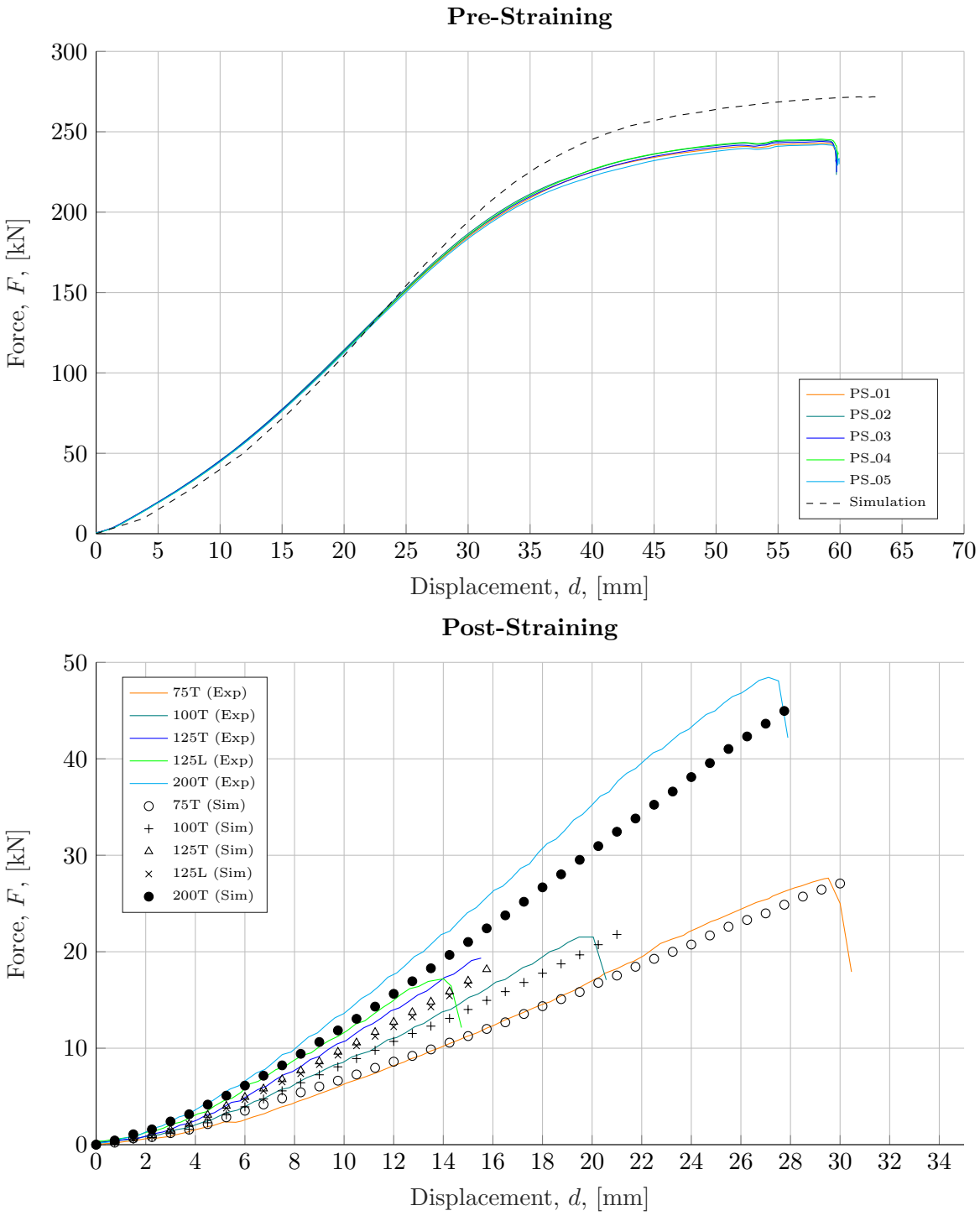


**Figure 5:** Comparison of experimental and simulated force-displacement curves for the pre- and post-straining operations.

was performed a step *after* where the effective plastic strain was determined corresponding to roughly a difference of 0.75 [mm] in punch displacement. Lastly, the material flow direction $\alpha$ was determined as the relationship between the minor and major strain increment from the end of the pre-straining operation to the end of the post-straining increment, with the exception of the 125L sample. For this sample, the $\alpha$-value is determined as the ratio between major and minor strain due to the radical turn of the strain path, practically meaning that for the post-straining, major strain becomes minor and vice versa. For the determination of the material flow direction, the experimental values are used. The values identified for the different samples for the material flow direction, effective plastic strain, and Advanced Formability state can be found in Table 4.

**Table 4:** Values of material flow direction ($\alpha$), effective plastic strain ($\bar{\varepsilon}^p$) and AutoForm™ R10 Advanced Formability. The effective plastic strain and Advanced Formability values are obtained from simulation, and the material flow direction is calculated based on experimental values. 'Excessive Thinning' is defined according to Volvo Cars standard.

| | **Pre-Strain** | **75T** | **100T** | **125T** | **125L** | **200T** |
|---|---|---|---|---|---|---|
| $\alpha$ | -0.644 | -0.396 | -0.103 | 0.085 | 0.038 | 0.958 |
| $\bar{\varepsilon}^p$ | 0.293 | 0.457 | 0.364 | 0.368 | 0.341 | 0.637 |
| Advanced Formability | Safe | Safe | Safe | Safe | Safe | Excess Thinning |

For the investigated approach, a transformation of the FLC into the alternative evaluation space is needed. The work presented in [5] investigated the same VDA239 CR4 mild steel and how sensitive the transformation was to the choice of material model. It was concluded that the transformation could not be decoupled from the choice of material model used in the simulation, why a transformation based on the BBC2005 material model was needed for this study, and the curve presented in [5] was adopted. Combining the curve with the information presented in Table 4, the failure evaluation in the alternative evaluation space displayed in Figure 6 can be created.

The results presented in Figure 6 provide an accurate failure prediction for four out of the five pre-strained Nakajima tests. For this initial investigation, the method fails to predict the failure for the 200T Nakajima sample, which is captured by the Advanced Formability functionality in AutoForm™ R10. The four pre-strained Nakajima samples accurately predicted (75T, 100T, 125T, and 125L) were all predicted safe by the Advanced Formability functionality. At first glance, the investigated methodology seems to be an improvement. This statement seems to be further strengthened by the fact that the Advanced Formability functionality does not account for load path changes with respect to the rolling direction, and this exact phenomenon was captured by the investigated approach.

## 4. Discussion

The investigated approach for failure prediction of the bi-linear strain paths proved to perform well for four out of the five pre-strain Nakajima specimens. For the 200T specimen geometry, the Advanced Formability functionality in AutoForm™ R10 predicted the onset of necking, however this is most likely a false positive. The first indication of failure occurs at a punch depth of 16.5 [mm] which is approximately 3.75 [mm] before the failure is determined in the experimental setup. Observing Figure 3 it can be found that the new necking limit for the pre-strain biaxial point is located above the original FLC, which might have let to the false positive identification of failure in the 200T sample.

As for the investigated approach's inability to predict the failure for the 200T sample, several reasons could be causing this. One obvious area of improvement that must be dealt

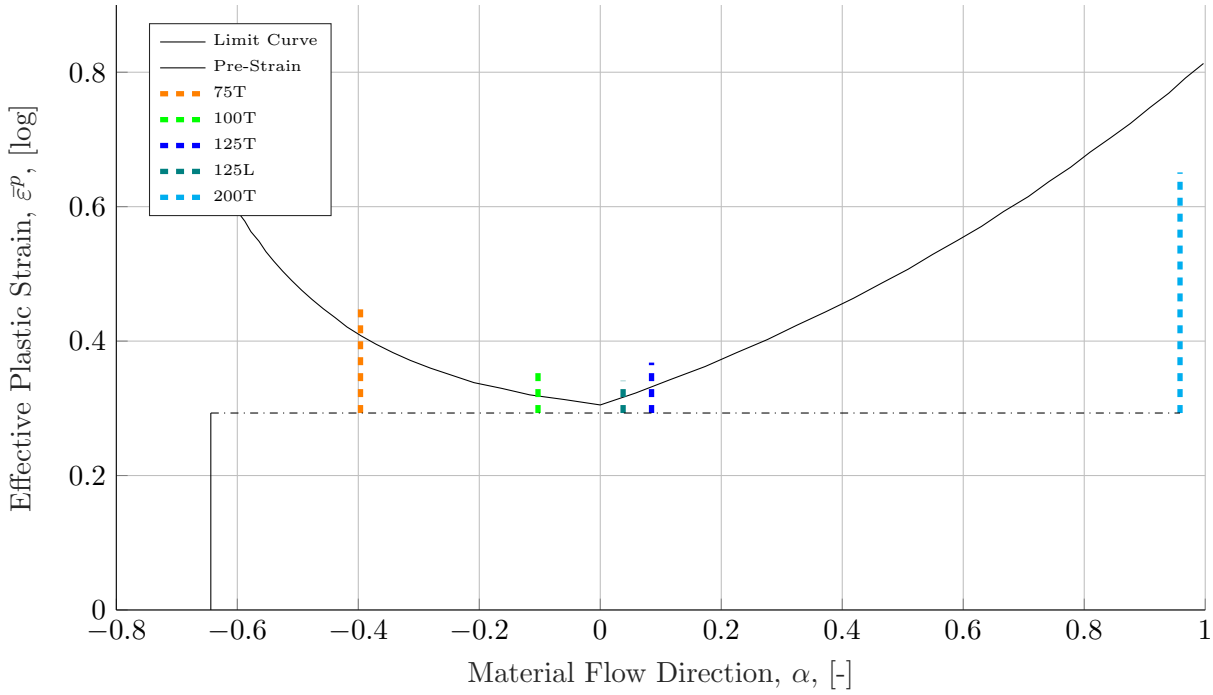


**Figure 6:** Failure assessment of the five pre-strained Nakajima samples in the alternative evaluation space proposed by Zeng et al. [8].

with in further investigations is a more accurate fit between the experimental and simulated force-displacement curves. Particularly the 200T sample displays a sub-par fit between the experimental and simulated curve which potentially impacts the strain predictions of the simulation. To obtain a better agreement between the experimental and simulated curve, several parameters could be investigated such as modifying the hardening curve (i.e. perform a power law extrapolation), the implementation of a strain rate sensitive hardening model, or modifications to the biaxial point of the yield locus.

In the presented work, the material flow direction $\alpha$ determined for each Nakajima sample was based on the experimentally obtained values. This choice was made as the material card applied to the Finite Element model was a slightly modified library card. This also means that the presented approach is in its current form not ready to be implemented in code as a post-processing technique, but further investigation into the method with more advanced models must be made.

## 5. Conclusion

The presented work introduced a new tool geometry for pre-straining of sheets. The work presented the results of five pre-strained samples that shows a stable pre-straining process in a single direction. The design of the tool allowed for a subsequent trimming operation producing Nakajima specimens of various width for the characterization of necking limits.

Following the successful pre-straining operation, five Nakajima tests were performed on sample widths of 75, 100, 125, and 200 transverse to the rolling direction, and a sample with width 125 along the rolling direction of the sheet. In an effort to accurately predict the failure in the pre-strained Nakajima tests, an approach using an alternative path independent evaluation space was used. This evaluation yielded an accurate prediction of failure in four of the five Nakajima tests, most notably an accurate prediction of the 125 sample in the longitudinal

direction, with a radical change in the loading direction.

**Acknowledgments**
Open Access funding was provided by Blekinge Institute of Technology. This study was also funded by VINNOVA in the Sustainable Production sub-program within Vehicle Strategic Research and Innovation (FFI) program (grant number 2020-02986).

## References

[1] Stoughton, T. 2000 A general forming limit criterion for sheet metal forming *Int. J. Mech. Sci.* **42** pp. 1-27.
[2] Volk, W. and J. Suh 2013 Prediction of formability for non-linear deformation history using generalized forming limit concept (GFLC) *AIP Conference Proceedings* **1567** pp. 556-561.
[3] Mattiasson, K., J. Jergéus, and P. DuBois 2014 On the prediction of failure in metal sheets with special reference to strain path dependence *Int. J. Mech. Sci* **88** pp. 175-191.
[4] Norz, R., N. Manopulo, M. Sigvant, A. R. Chezan and W. Volk 2022 Prediction of necking initiation in case of abrubt changes in the loading direction *The Minerals, Metals & Materials Series: NUMISHEET 2022* pp. 617-625.
[5] Barlo, A., M. Sigvant, N Manopulo, M. S. Islam. and J. Pilthammar 2022 Failure prediction of automotive components utilizing a path independent forming limit criterion *Key Engineering Materials* **926** pp. 906-916.
[6] International Standard Organization 2008 Metallic Materials - sheet and strip - Determination of forming-limit-curves (ISO 12004-2).
[7] Sigvant, M., K. Mattiasson and M. Larsson 2008 The definition of incipient necking and its impact on experimentally or theoretically determined forming limit curves *IDDRG 2008 Conference Proceedings*.
[8] Zeng, D., L. Chappuis, Z. C. Xia and X. Zhu 2009 A path independent forming limit criterion for sheet metal forming simulations *SAE Int. J. Mater. Manu.* Vol. 1, No. 1, pp. 809-817.
[9] Pilthammar, J., D. Banabic and M. Sigvant 2021 BBC05 with non-integer exponent and ambiguities in nakajima yield surface calibration *Int. J. Mater. Form.* **14**, pp. 577-592.